

Article

Evaluation of Half-Cell Potential Measurements for Reinforced Concrete Corrosion

Yousef Almashakbeh ^{1,*} , Eman Saleh ²  and Nabil M. Al-Akhras ³

¹ Department of Allied Engineering Sciences, Faculty of Engineering, The Hashemite University, P.O. Box 330127, Zarqa 13133, Jordan

² Civil Engineering Department, Faculty of Engineering, The Hashemite University, P.O. Box 330127, Zarqa 13133, Jordan; emanf_yo@hu.edu.jo

³ Civil Engineering Department, Jordan University of Science and Technology, P.O.Box 3030, Irbid 22110, Jordan; alakhras@just.edu.jo

* Correspondence: yousefalmashakbeh@hu.edu.jo

Abstract: The evaluation of half-cell potential measurements in reinforced concrete (RC) members can be a key issue for civil engineers. The primary reason for this is that the interpretation of half-cell potential measurements based on the available standards provides information related only to the possibility of corrosion in concrete, but it does not provide a clear perception of the influence of corrosion on the capacity of the RC members. The objective of this study is two-fold: (1) to explore the influence of corrosion level on the flexural capacity of RC members; and (2) to provide engineers with a better understanding of the correlation between half-cell potential measurements and flexural capacity of RC members. To establish this, twelve RC beams were cast and then exposed to accelerated corrosion utilizing an impressed current. After that, half-cell potential tests were performed on the entire surface of the beams. Next, a four-point loading test was performed on the beams to determine their flexural behavior. The analysis of measurements showed that there is a high positive correlation between the half-cell potential measurements and the flexural capacity of the tested beams which demonstrates the potential of half-cell measurements to predict the capacity degradation level of the RC beams due to corrosion.

Keywords: corrosion; half-cell potential; ductility; flexural capacity



Citation: Almashakbeh, Y.; Saleh, E.; Al-Akhras, N.M. Evaluation of Half-Cell Potential Measurements for Reinforced Concrete Corrosion. *Coatings* **2022**, *12*, 975. <https://doi.org/10.3390/coatings12070975>

Academic Editors: Junjie Wang and Hongwei Lin

Received: 2 June 2022

Accepted: 6 July 2022

Published: 9 July 2022

Publisher's Note: MDPI stays neutral with regard to jurisdictional claims in published maps and institutional affiliations.



Copyright: © 2022 by the authors. Licensee MDPI, Basel, Switzerland. This article is an open access article distributed under the terms and conditions of the Creative Commons Attribution (CC BY) license (<https://creativecommons.org/licenses/by/4.0/>).

1. Introduction

Degradation of structures due to corrosion of embedded steel is considered one of the major durability problems faced by the construction industry [1–5]. The rate of steel corrosion is increased by the ingress of either chloride ion (Cl^-) or CO_2 into concrete, reducing the alkaline hydrated cement products that passivate (i.e., shield) the embedded steel. Corrosion causes a reduction in the cross-section of embedded steel, thereby reducing its flexural and tensile strength capacities [6,7]. This could cause the development of many cracks on the concrete that, in turn, reduce the load capacity of the structure.

The *NACE* (2013) impact study reported that the estimated cumulative cost of corrosion was approximately 4% of the global gross domestic product. Further, it reported that the utilization of corrosion prevention practices may yield a reduction in the cost by 15–35% [8]. The deteriorated structures due to corrosion may require a higher cost for rehabilitation than the cost of initial construction [9–11]. Moreover, the corrosion of embedded steel could increase the risk of failure due to the presence of external forces such as earthquakes. Therefore, an early detection and assessment of reinforced concrete (RC) corrosion are necessary to accelerate corrective measures [12,13]. This assessment should provide information regarding the remaining service life, level of damage, and required repairs [14,15].

The half-cell potential method is a commonly applied technique for detecting corrosion in RC members [16,17]. This technique is performed and interpreted based on ASTM C876 standards [18]. It measures the value of potential on the surface of concrete members where the positive pole of the high-impedance voltmeter is electrically attached to the reinforcing steel and the other pole is attached to a reference electrode. The measured potential is then translated into the risk of corrosion of embedded steel inside the RC members [1,19]. Table 1 shows the criteria followed to interpret the potential values for corrosion detection. For example, when the potential value is less than -200 mV, the reinforced steel is categorized to have a low risk of corrosion (i.e., less than 10% risk level).

Table 1. Corrosion activity according to half-cell values (ASTM C876).

Half-Cell Potential Values	Probability of Corrosion
less negative than -200 mV	10% probability of corrosion
between -200 mV and -350 mV	Approximately 50%
more negative than -350 mV	90% probability of corrosion

Few studies have considered the half-cell potential test as an indicator of corrosion in embedded reinforcing bars. Jung et al. [11] and Gonzalez et al. [20] performed an experimental study to evaluate the structural performance of corrosion-damaged RC beams. In their study, it was concluded that corrosion adversely affects the ultimate load and energy dissipation capacity of RC members and they suggested further experimentation for evaluating the performance of structures with corrosion-damaged members. Naish et al. [21] and Pradhan and Bhattacharjee [22] tried to link the potential and resistivity measurements to the corrosion of RC members. According to these studies, a strong correlation between the half-cell potential measurements and the corrosion level was observed; however, they did not link the half-cell potential measurements to the performance degradation level of corrosion-damaged members. Adriman et al. [19] showed, using a case study, that a half-cell potential test augmented with computational approaches is a promising method to improve the diagnosis of corrosion in RC members. Thus, Adriman et al. [19] demonstrated that half-cell potential measurements can be used beyond the qualitative corrosion risk assessment established by the ASTM C876 [18] (see Table 1).

In this study, the objective is to quantify the impact of corrosion on the flexural behavior of RC beams and link it to half-cell potential measurements. This link will help to expand the usability of half-cell potential measurements to quantitatively predict the degree of degradation of corrosion-damaged members. In addition, the effectiveness of half-cell potential measurements as corrosion indicators will be investigated through this established link.

2. Experimentation

Figure 1 illustrates the process followed to prepare the control beams and corroded beams used to establish the link between the flexural behavior of corrosion-damaged beams and half-cell potential measurements. As shown in Figure 1, first, the concrete mixture and reinforced cage were designed, based on the ACI-211 guidelines [23] and ACI 318 standards [24], respectively. After that, the mixture was prepared, tested for workability and strength (i.e., slump and cube test, respectively), and cast into forms. To induce corrosion, an electrically impressed current was used. After prespecified durations, half-cell potential tests were performed on the entire surface of the beams. Then, a four-point loading test was conducted to estimate the impact of corrosion on the flexural behavior of RC beams. Finally, the link was established by a comparison between the strength-deformation properties of corroded beams, obtained from the four-point loading test, and the half-cell potential measurements. The following is a detailed description of each step illustrated in Figure 1.

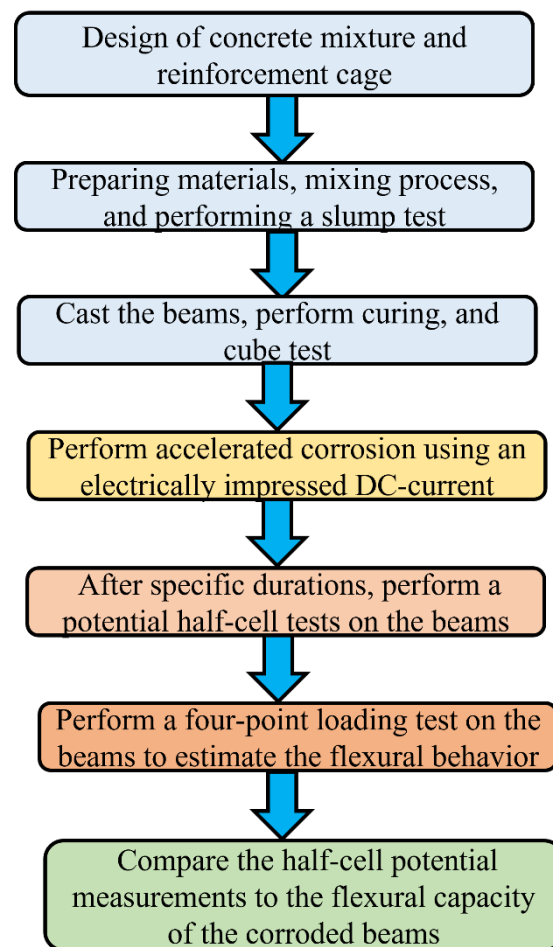


Figure 1. Schematic flow chart used for the evaluation of half-cell potential measurement.

2.1. Material

The concrete mix was designed following the ACI-211 guidelines [23], with a water-to-cement ratio of 0.47. The RC beams were prepared using ordinary Portland cement (Type I) with coarse limestone aggregates of 12.5 mm, in addition to a mixture of silica sands and crushed fine limestone (20% silica and 80% fine aggregate). The ASTM standard technique C136 was used to determine the fineness modulus of fine limestone. Following the ASTM C127 method, the saturated surface dry (SSD) bulk specific gravity (BSG) and absorption of coarse limestone aggregate were 2.56 and 1.34%, respectively. Moreover, according to ASTM C128, the bulk specific gravity (SSD) and absorption of fine limestone aggregate were 2.52 and 3.41%, respectively. For silica sand, the corresponding percentages were 2.59 and 0.73%. Further, as per ASTM C29, the unit weight for coarse aggregate was 1362 kg/m³. The beam reinforcements were constructed using two distinct grades of steel reinforcement: G40 and G60. The mechanical characteristics of the steel reinforcements are listed in Table 2.

Table 2. Mechanical properties of steel reinforcement.

Size	Grade	Yield Strength, F_y (MPa)	Ultimate Strength, F_u (MPa)	Elongation %
6 mm	G40	290	353	14
10 mm	G60	441.8	657	12.9
12 mm	G60	435.5	631	14.7
14 mm	G60	463	640	16

2.2. Test Specimens

Twelve reinforced concrete beams with dimensions $150 \times 100 \times 1000$ mm were tested. All rebars were 12 mm in diameter and embedded at 35 mm cover thickness from the surface. Stirrups with a spacing of 50 mm were provided along the length of the beam. Internally dimensioned wooden molds were constructed and used to cast the test specimens. Before concrete casting, the steel reinforcement was assembled and placed within the molds in the shape of a cage. Three beams and three cylinders (100×200 mm) were cast in each batch to be tested for compressive strength, which was determined to be around 41.6 MPa. A tilting drum mixer with a batch volume of approximately a quarter m^3 was used. The slump was tested (per ASTM-C143) and determined to be about 50 mm. Three layers of fresh concrete were poured into the wooden molds. Each layer was vibrated on a compacting table. After 24 h, the beam specimens were demolded and cured for 28 days with wet burlap. Figure 2 shows the above steps.

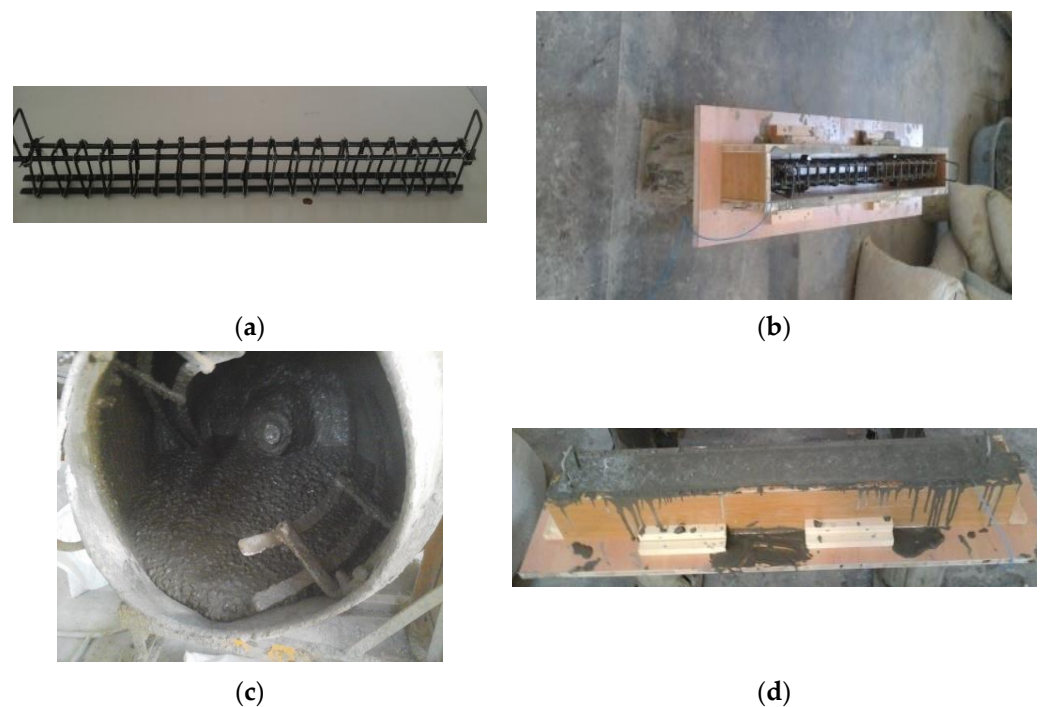


Figure 2. Steps for preparation of test specimens. (a) A typical steel reinforcement. (b) Steel reinforcement cage inside the wooden mold. (c) Mixing of concrete ingredients. (d) Casted specimens.

2.3. Corrosion Process

The electrically impressed DC was used to accelerate the corrosion process on the RC beams. The accelerated corrosion process was achieved by applying DC (direct current) to both the longitudinal steel bars and stirrups, which serve as anodes within each beam through metallic wires put before casting. The cathode was constructed using a steel plate with a dimension of $(800 \times 300 \times 10)$ mm that was linked to the cathode wire. The specimens were subjected to a $200 \mu\text{A}/\text{cm}^2$ current density. To create an aggressive environment, samples were put in a tank containing a solution of NaCl at a concentration of 2%, as illustrated in Figure 3.



Figure 3. The accelerated corrosion process. (a) Three days of accelerated corrosion. (b) Eight days of accelerated corrosion.

2.4. Half-Cell Potential Test

Nondestructive tests were used to analyze the physical qualities of concrete, such as discontinuities and changes in the composition of concrete and corrosion level, without causing any damage to the tested specimens. Here, the half-cell potential test was performed on the cast RC beams. Each beam was split into ten sections. The half-cell potential equipment was used to collect three readings at each test location per the ASTM C876 [18] requirements. The measurement was performed using a silver/silver chloride reference electrode. Before the test, the beam was moistened with water to enhance the moisture content of the concrete. Then, a saturated sponge with alcohol was put on the concrete surface, followed by the reference electrode. The other end of the voltmeter was then linked to the steel rebar (see Figure 4).

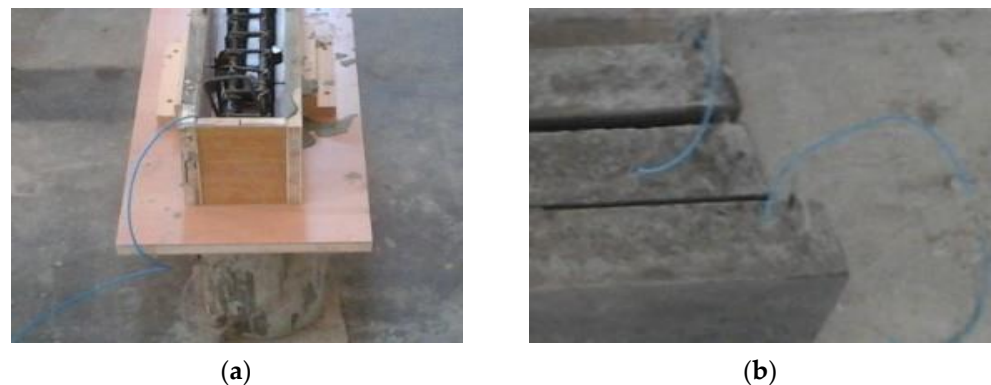


Figure 4. Connected wire with rebar. (a) Before casting. (b) After casting.

2.5. Flexural Behavior

Flexural testing was performed on the beams under four-point loading across a span of 0.9 m in a simple support arrangement. Between the two loading points, the spacing was 300 mm. The beam was supported by a special sort of support made of hardened steel to guarantee that no deformation occurred that might impact the test findings. All beams were loaded with two-point loads utilizing 400 kN hydraulic testing equipment at a loading rate of 0.3 kN/s. Supports were designed to function as a hinge on one end and a roller on the other. The vertical deflection at the mid-span was determined using a linear variable displacement transducer (LVDT). The load-deflection curves were constructed using the data obtained from the load cell and LVDT. The test setup is illustrated in Figure 5.



Figure 5. The test set-up used.

3. Experimental Results and Discussion

This section presents and discusses the experimental results of the performed experiments. An evaluation of half-cell potential measurements was performed by comparison with the flexural capacity of the corrosion-damaged RC beams.

In the tests, all the beams (i.e., uncorroded and corroded) initially developed flexural cracks in the high moment zone region (see Figure 6), which subsequently expanded into the compression zone and propagated across the shear span as the load increased. Before collapsing, the cracks expanded deep into the compression zone. As shown in Figure 6, the crack patterns for both the control beams and corroded beams were very similar and exhibited a ductile failure (i.e., flexural failure).

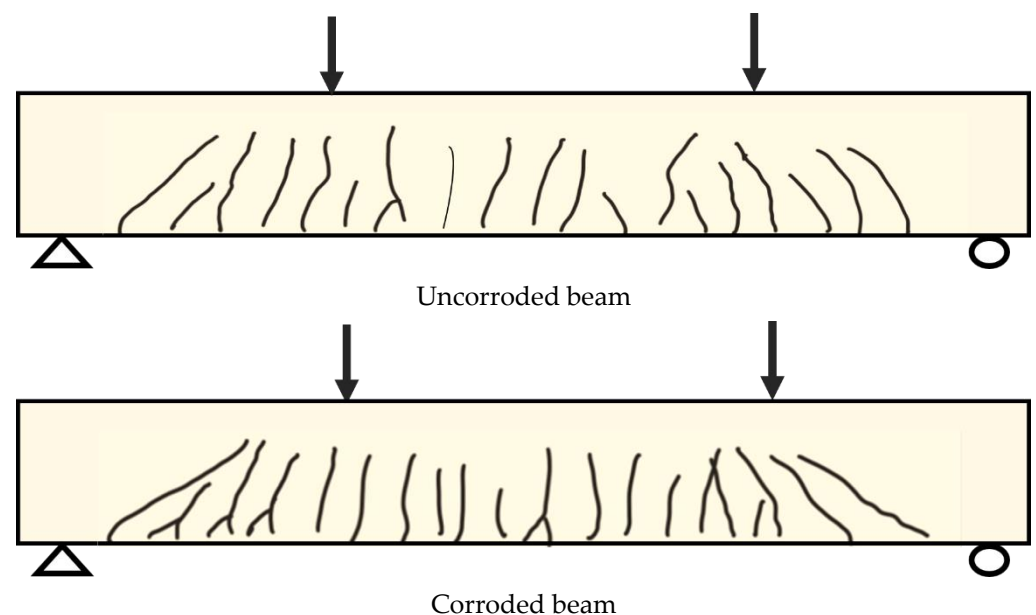


Figure 6. Crack patterns of the uncorroded and corroded beam.

The load and vertical deflection of the beams were recorded and plotted for each specimen during the test. These curves were then investigated based on their initial stiffness, maximum displacement, maximum load, and toughness.

3.1. Flexural Behavior

The mechanical response of the beams was determined using load-deflection curves and their related properties, including maximum displacement, maximum load, initial stiffness, and toughness. The load-deflection curves and the average features of the curves of six of the twelve tested corroded beams and their corresponding uncorroded RC beam

(i.e., control beams) are illustrated in Figure 7 and Table 3, respectively. As shown in Figure 7, the curves exhibited linear behavior during the first phase of loading before showing a nonlinear behavior. All the corroded beams were found to have a lower ultimate capacity than the control beams. The average load capacity of all corroded beams was computed to be 84% of the control beams. In addition, the average ductility of corroded beams was estimated to be 114.4% of the average ductility of the corresponding control beams. All corroded RC beams had a greater stiffness than uncorroded beams; the corroded beams retained 111% of their original stiffness. These observations are similar to the results observed in [11,20] where it was concluded that corrosion adversely affects the flexural capacity of RC beams.

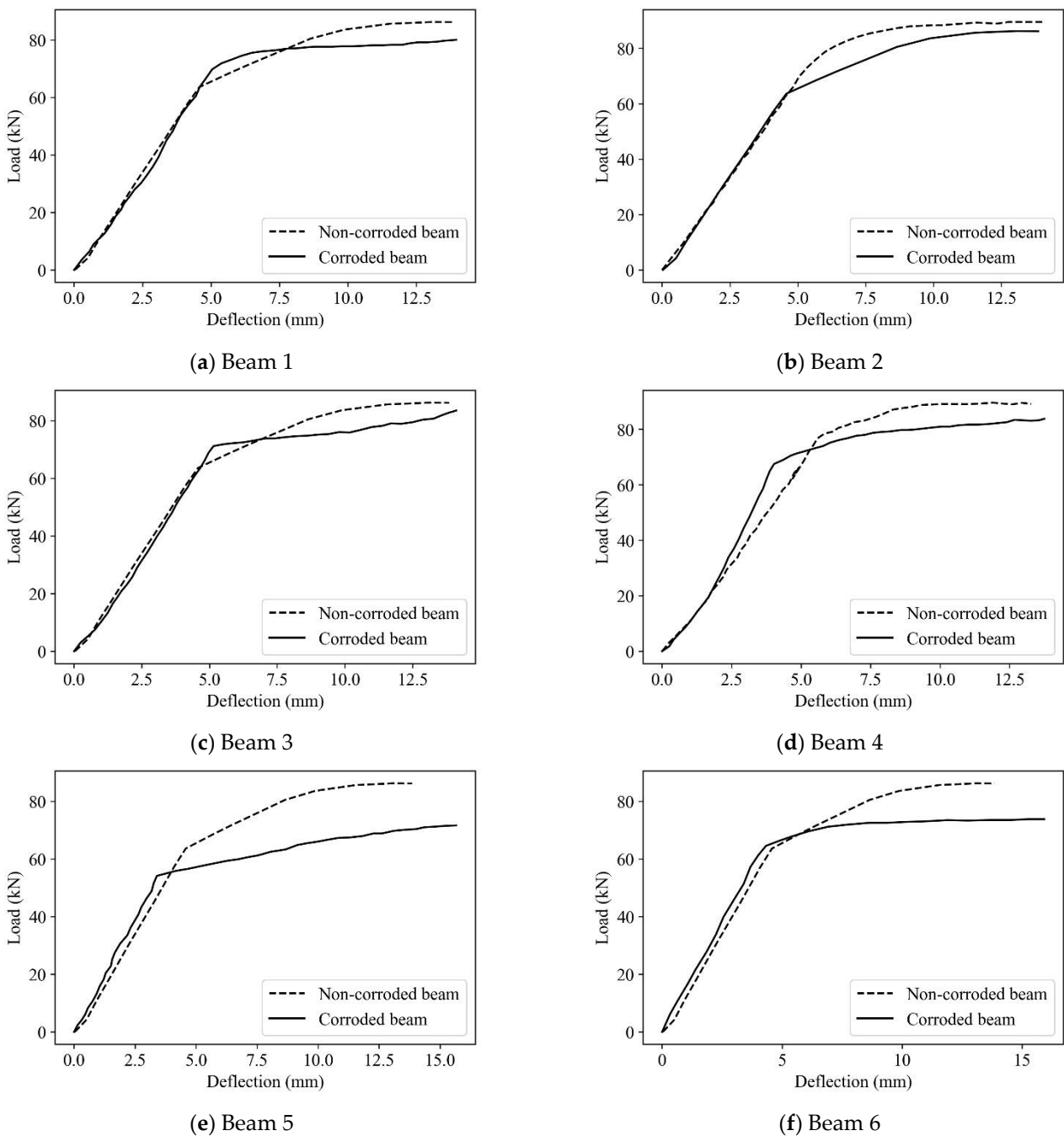


Figure 7. Load–deflection curves for the RC beams.

Table 3. The average mechanical characteristics for control and corroded beams.

Case	Beam Designation	Ultimate Load (kN)	Max Deflection (mm)	Toughness (J)	Stiffness (MN/m)
1	Control beam	86.2	13.9	877.5	13.75
2	Corroded beams	72.7 (84%)*	15.80 (114%)*	928.0 (106%)*	15.21 (111%)*

* Residual properties.

3.2. Analysis of Half-Cell Potential Measurements

Figure 8 illustrates the half-cell potential values for one of the tested RC beams before and after corrosion exposure. Before corrosion, all beams had values less than -200 mV, indicating a low possibility of corrosion (see Table 1). However, after corrosion, the half-cell potential measurements increased drastically, exceeding -350 mV, indicating the presence of considerable corrosion. The other tested RC beams showed similar behavior to the one in Figure 8.

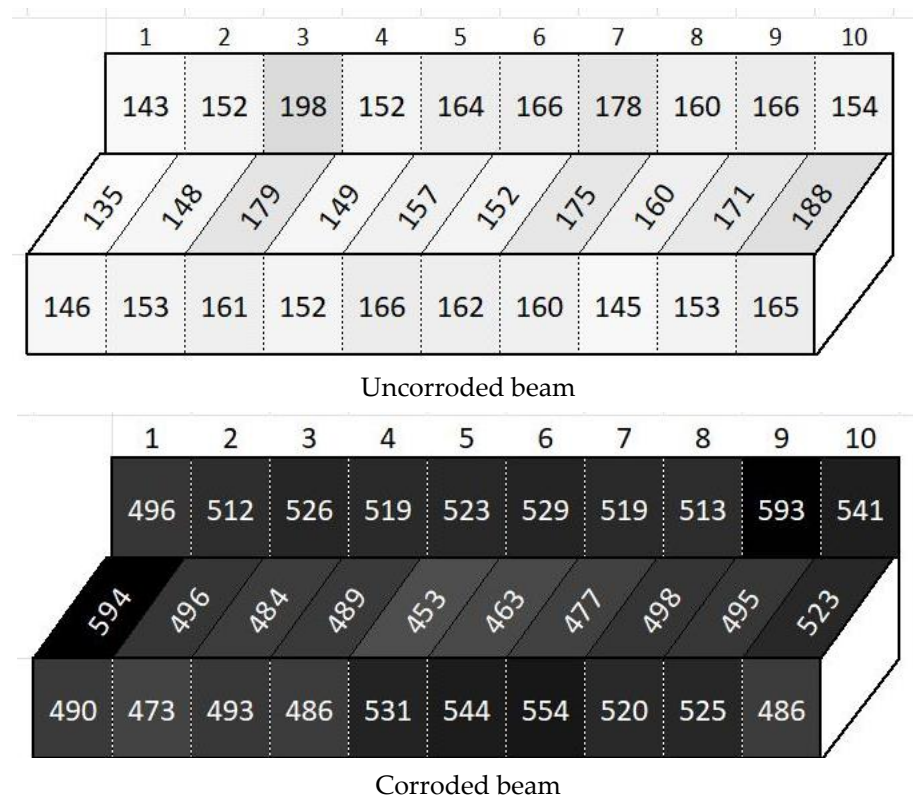


Figure 8. Half-cell potential measurements of the corroded beams after 8 days of corrosion and the corresponding uncorroded one.

3.3. Correlation between Half-Cell Potential Measurements and Four-Point Loading Test

Performing a correlation study between the half-cell potential measurements and the four-point loading test resulted in a negative correlation between the half-cell potential measurements and the ultimate load capacity of corroded RC beams and a positive correlation between the half-cell potential measurements and the ductility of half-cell potential measurements. A Pearson’s correlation coefficient of -0.93 indicated a high correlation between the half-cell potential measurements and flexural capacity of RC beams, while a Pearson’s correlation coefficient of 0.74 between the half-cell potential measurements and ductility of the beams implied a high-to-moderate correlation between the results.

4. Conclusions and Recommendations for Future Research

In this study, the effect of corrosion of embedded steel on the flexural behavior of RC beams and the level of correlation between half-cell potential measurements and the flexural behavior of RC beams were investigated. The following results can be drawn from the experimental investigation:

- The objective of this study was to provide a better understanding of the strength-deformation behavior of corroded members. Based on the test results, it was observed that the failure patterns of the corroded beams were generally similar to the control beams. However, it was observed that the ultimate capacity of the RC beams decreased, while the stiffness and ductility increased with the duration of accelerated corrosion.
- The ductility increased with increasing half-cell potential, while the flexural capacity decreased with increasing half-cell potential. The increase in ductility was 114.4% of residual deflection and the decrease in flexural capacity was 16% lower than that of control beams at the maximum half-cell potential.
- We observed a relatively strong correlation between the average potential difference and the degradation in the flexural capacity of the beams (Pearson's correlation = 0.93). Thus, the potential difference can be used as an indicator of the degradation level in RC members.
- To propose a practical procedure for evaluating the flexural capacity of corroded members using half-cell potential measurements, further experimental research on corroded members, together with analytical analysis such as finite element analysis, should be performed. This practical procedure may aspire to derive a degradation factor formula that uses half-cell potential measurements to predict the capacity of corrosion-damaged members.

Author Contributions: Conceptualization, Y.A.; data curation and elaboration, E.S.; experimental tests, Y.A.; validation and writing, Y.A., E.S. and N.M.A.-A. All authors have read and agreed to the published version of the manuscript.

Funding: This research was funded by the Deanship of Scientific Research at Jordan University of Science and Technology (Project 100/2016).

Institutional Review Board Statement: Not applicable.

Informed Consent Statement: Not applicable.

Data Availability Statement: The data is available upon reasonable request from the authors.

Conflicts of Interest: The authors declare no conflict of interest.

References

1. Yodsudjai, W.; Pattarakittam, T. Factors influencing half-cell potential measurement and its relationship with corrosion level. *Measurement* **2017**, *104*, 159–168. [[CrossRef](#)]
2. Qiao, G.; Hong, Y.; Ou, J. Quantitative monitoring of pitting corrosion based on 3-D cellular automata and real-time ENA for RC structures. *Measurement* **2014**, *53*, 270–276. [[CrossRef](#)]
3. Li, C.; Chen, Q.; Wang, R.; Wu, M.; Jiang, Z. Corrosion assessment of reinforced concrete structures exposed to chloride environments in underground tunnels: Theoretical insights and practical data interpretations. *Cem. Concr. Compos.* **2020**, *112*, 103652. [[CrossRef](#)]
4. Abouhussien, A.A.; Hassan, A.A.A. Acoustic emission monitoring of corrosion damage propagation in large-scale reinforced concrete beams. *J. Perform. Constr. Facil.* **2018**, *32*, 4017133. [[CrossRef](#)]
5. Deng, H.; Zhu, P.; Hu, C.; He, T. Study on Dynamic Lubrication Characteristics of the External Return Spherical Bearing Pair under Full Working Conditions. *Machines* **2022**, *10*, 107. [[CrossRef](#)]
6. Zhou, Y.; Gencturk, B.; Willam, K.; Attar, A. Carbonation-induced and chloride-induced corrosion in reinforced concrete structures. *J. Mater. Civ. Eng.* **2015**, *27*, 4014245. [[CrossRef](#)]
7. Meng, D.; Lin, S.; Azari, H. Nondestructive corrosion evaluation of reinforced concrete bridge decks with overlays: An experimental study. *J. Test. Eval.* **2019**, *48*, 516–537. [[CrossRef](#)]
8. Koch, G.; Varney, J.; Thompson, N.; Moghissi, O.; Gould, M.; Payer, J. International measures of prevention, application, and economics of corrosion technologies study. *NACE Int.* **2016**, *216*, 2–3.

9. Qiao, G.; Hong, Y.; Ou, J. Corrosion monitoring of the RC structures in time domain: Part I. Response analysis of the electrochemical transfer function based on complex function approximation. *Measurement* **2015**, *67*, 78–83. [[CrossRef](#)]
10. Zhang, J.; Liu, C.; Sun, M.; Li, Z. An innovative corrosion evaluation technique for reinforced concrete structures using magnetic sensors. *Constr. Build. Mater.* **2017**, *135*, 68–75. [[CrossRef](#)]
11. Jung, J.-S.; Lee, B.Y.; Lee, K.-S. Experimental study on the structural performance degradation of corrosion-damaged reinforced concrete beams. *Adv. Civ. Eng.* **2019**, *2019*, 1–14. [[CrossRef](#)]
12. Fonna, S.; Huzni, S.; Ridha, M.; Ariffin, A.K. Inverse analysis using particle swarm optimization for detecting corrosion profile of rebar in concrete structure. *Eng. Anal. Bound. Elem.* **2013**, *37*, 585–593. [[CrossRef](#)]
13. Fonna, S.; Huzni, S.; Ariffin, A.K. Boundary element inverse analysis for rebar corrosion detection: Study on the 2004 tsunami-affected structure in Aceh. *Case Stud. Constr. Mater.* **2018**, *8*, 292–298. [[CrossRef](#)]
14. Saleh, E.; Tarawneh, A.; Dwairi, H.; AlHamaydeh, M. Guide to non-destructive concrete strength assessment: Homogeneity tests and sampling plans. *J. Build. Eng.* **2022**, *49*, 104047. [[CrossRef](#)]
15. Saleh, E.F.; Tarawneh, A.N.; Katkhuda, H.N. A comprehensive evaluation of existing and new model-identification approaches for non-destructive concrete strength assessment. *Constr. Build. Mater.* **2022**, *334*, 127447. [[CrossRef](#)]
16. Amiri, A.S.; Erdogmus, E.; Richter-Egger, D. A Comparison between Ultrasonic Guided Wave Leakage and Half-Cell Potential Methods in Detection of Corrosion in Reinforced Concrete Decks. *Signals* **2021**, *2*, 413–433. [[CrossRef](#)]
17. Reddy, V.S.; Naidu, K.S.S.T.; Rao, M.V.S.; Shrihari, S. Electrical Resistivity and Half-Cell Potential Studies to assess organic and inorganic corrosion inhibitors' effectiveness in concrete. *E3S Web Conf.* **2020**, *184*, 1082. [[CrossRef](#)]
18. *ASTM C876-15*; Standard Test Method for Corrosion Potentials of Uncoated Reinforcing Steel in Concrete. ASTM International: West Conshohocken, PA, USA, 2016.
19. Adriman, R.; Ibrahim, I.B.M.; Huzni, S.; Fonna, S.; Ariffin, A.K. Improving half-cell potential survey through computational inverse analysis for quantitative corrosion profiling. *Case Stud. Constr. Mater.* **2022**, *16*, E00854. [[CrossRef](#)]
20. Gonzalez, J.A.; Miranda, J.M.; Feliu, S. Considerations on reproducibility of potential and corrosion rate measurements in reinforced concrete. *Corros. Sci.* **2004**, *46*, 2467–2485. [[CrossRef](#)]
21. Naish, C.C.; Harker, A.; Carney, R.F.A. Concrete inspection: Interpretation of potential and resistivity measurements. Corrosion of reinforcement in concrete. In Proceedings of the Third International Symposium on “Corrosion of Reinforcement in Concrete Construction”, Wishaw, UK, 21–24 May 1990; CICC Publisher: UK, 1990.
22. Pradhan, B.; Bhattacharjee, B. Half-cell potential as an indicator of chloride-induced rebar corrosion initiation in RC. *J. Mater. Civ. Eng.* **2009**, *21*, 543–552. [[CrossRef](#)]
23. ACI Committee. ACI Committee 211. In *Standard Practice for Selecting Proportions for Normal, Heavyweight and Mass Concrete (Reapproved 2009)*; ACI Committee: Farmington Hills, MI, USA, 2009.
24. ACI Committee. *Building Code Requirements for Structural Concrete (ACI 318-19) and Commentary*; ACI Committee: Farmington Hills, MI, USA, 2019.